Undersulfated and Glycol-Split Heparins Endowed with Antiangiogenic Activity

Benito Casu,*,† Marco Guerrini,† Sara Guglieri,† Annamaria Naggi,† Marta Perez,† Giangiacomo Torri,† Giuseppe Cassinelli,† Domenico Ribatti,‡ Paolo Carminati,§ Giuseppe Giannini,§ Sergio Penco,§ Claudio Pisano,§ Mirella Belleri,|| Marco Rusnati,|| and Marco Presta||

G. Ronzoni Institute for Chemical and Biochemical Research, 20133 Milan, Italy, Department of Anatomy, University of Bari, 70212 Bari, Italy, and Sigma-Tau Research Department, 0040 Pomezia, Rome, Italy, and Unit of General Pathology and Immunology, Department of Biomedical Sciences and Biotechnology, School of Medicine, University of Brescia, 25123 Brescia, Italy

Received May 8, 2003

Tumor neovascularization (angiogenesis) is regarded as a promising target for anticancer drugs. Heparin binds to fibroblast growth factor-2 (FGF2) and promotes the formation of ternary complexes with endothelial cell surface receptors, inducing an angiogenic response. As a novel strategy to generate antiangiogenic substances exploiting binding to FGF2 while preventing FGF receptor (FGFR) activation, sulfation gaps were generated along the heparin chains by controlled alkali-catalyzed removal of sulfate groups of iduronic acid 2-*O*-sulfate residues, giving rise to the corresponding epoxide derivatives. A new class of heparin derivatives was then obtained by opening the epoxide rings followed by oxidative glycol-splitting of the newly formed (and the preexisting) nonsulfated uronic acid residues. In vitro these heparin derivatives prevent the formation of FGFR/FGF2/heparan sulfate proteoglycan ternary complexes and inhibit FGF2-stimulated endothelial cell proliferation. They exert an antiangiogenic activity in the chick embryo chorioallantoic membrane assay, where the parent heparin is inactive. Low and very low molecular weight derivatives of a prototype compound, as well as its glycine and taurine derivatives obtained by reductive amination of glycol-split residues, retained the angiostatic activity. A significant relationship was found between the extent of glycol-splitting and the FGF2-antagonist/angiostatic activities of these heparin derivatives. Molecular dynamics calculations support the assumption that glycol-split residues act as flexible joints that, while favoring 1:1 binding to FGF2, disrupt the linearity of heparin chains necessary for formation of active complexes with FGFRs.

Introduction

Neovascularization (angiogenesis) is a pivotal step in tumor growth and metastasis and its inhibition is considered a promising target for anticancer drugs.[1] Heparin-binding endothelial growth factors, like members of the fibroblast growth factor (FGF) and vascular endothelial growth factor (VEGF) families, induce new blood vessel formation by activating their cognate tyrosine kinase receptors (FGFR) on the endothelial cell surface. Such an activation requires the formation of ternary complexes among the growth factor, its receptors, and the polysaccharide chains of heparan sulfate (HS) proteoglycans (HSPG).[2−4]

Heparin, a HS-like polysaccharide extracted from animal organs, is widely used in therapy as an anticoagulant and antithrombotic drug.[5] Retrospective studies indicated that heparin administered as antithrombotic to cancer patients has significantly increased survival times.[6] Beneficial effects of heparin in cancer are thought to be associated with the binding to and inhibition of one or more proteins overexpressed by tumor cells, including heparin-binding growth factors,[4] heparanase,[7] and platelet selectin.[8] However, the anticoagulant properties of heparin involve hemorragic risks, and studies have been addressed to generate nonanticoagulant variants of the polysaccharide endowed with potential antitumor properties.[9]

Like HS, heparin belongs to the family of glycosaminoglycans (GAG) and is constituted by repeating disaccharide units of uronic acid (β-D-glucuronic, GlcA, or α-L-iduronic, IdoA) and α-D-glucosamine (GlcN) residues. The common precursor of heparin and HS, *N*-acetyl heparosan (made up of repeating disaccharide units of GlcA and *N*-acetylated glucosamine, GlcNAc), undergoes biosynthetic modifications involving *N*-deacetylation (followed by *N*-sulfation) of the GlcN residues, C5-epimerization of GlcA, and *O*-sulfation (prevalently at position 2 of IdoA residues generated by epimerization of GlcA, and at position 6 of GlcN). These biosynthetic modifications are not evenly distributed along the GAG chain, which contains highly *O*-sulfated, prevalently *N*-sulfated (NS), undersulfated, prevalently *N*-acetylated (NA), and mixed (NA/NS) regions. Whereas the chains of heparins currently used in therapy are prevalently constituted of NS regions made up of repeating units of 2-*O*-sulfated IdoA ($IdoA2SO_3$) and *N*- and 6-*O*-sulfated GlcN ($GlcNSO_36SO_3$) (sequence **1** in Figure 1), HS has a more hybrid structure, with substantial proportions of NA and NA/NS regions containing nonsulfated uronic acid (mainly GlcA) and GlcNAc residues. A minor but important sequence of heparin (also

* Corresponding author. Phone: (+39) 02−7064 1623. Fax: (+39) 02−7064 1634. E-mail: casu@ronzoni.it.
† G. Ronzoni Institute for Chemical and Biochemical Research.
‡ University of Bari.
§ Sigma-Tau Research Department, University of Brescia.
|| Unit of General Pathology and Immunology, University of Brescia.

10.1021/jm030893g CCC: $27.50
Published on Web 01/08/2004

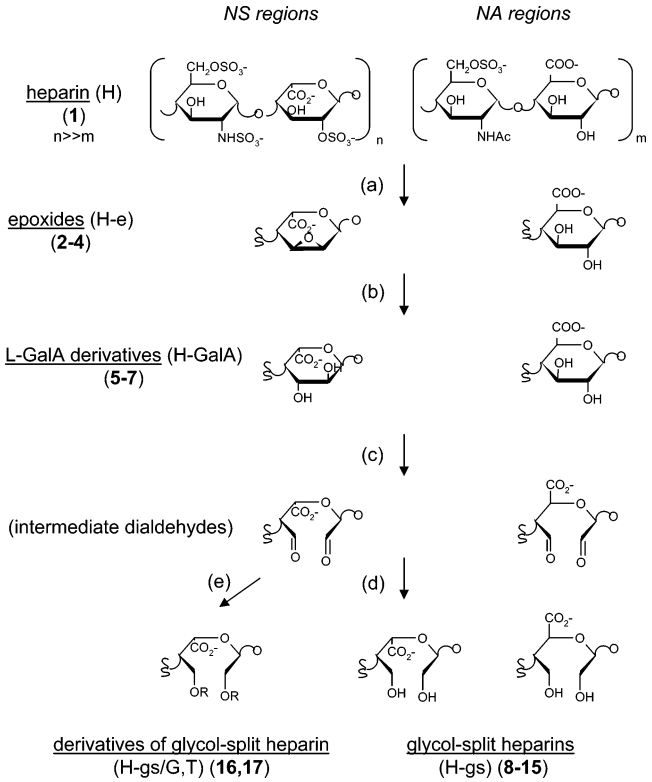

Figure 1. Structure of disaccharide units of heparin and modified uronic acid acid residues following (a) alkali treatment; (b) heating at 70 °C/pH 7, (c) reaction with periodate; (d) borohydride reduction of dialdehydes; (e) derivatization of dialdehydes with glycine (G) and taurine (T). Whereas all reactions involve L-iduronic acid residues of the prevalent, *N*-sulfated (NS) regions, glycol splitting modifies also D-glucuronic acid residues of the minor, *N*-acetylated (NA) regions.

represented, in even lower amounts, in HS) is a pentasaccharide containing a GlcA residue followed by a unique trisulfated GlcN residue ($GlcNSO_3 3,6SO_3$). This pentasaccharide is the active site for antithrombin and therefore a major determinant of the anticoagulant and antithrombotic properties of heparin. Being constituted by polysaccharide chains of different length, heparin is also size-heterogeneous and its structure can be described only in statistical terms. Most of the binding and biological properties of GAGs are size-dependent, and polydispersion of the molecular weights modulates the binding and biological properties of heparin and its derivatives.[10,11]

Fibroblast growth factor-2 (FGF2, formerly named "basic" FGF) is a major inducer of angiogenesis[12] and its activity is modulated by heparin. Exogenous heparin competes with HS chains of cell-surface HSPGs for binding FGF2.[13] Depending on their length, NS heparin sequences either inhibit or activate the growth factor. Chains constituting current heparins (including LMWHs) prevalently contain these "fully sulfated" sequences and are sufficiently long to bind more than one FGF molecule[13] and to organize FGF dimers and higher oligomers in such a way as to favor the formation of ternary complexes with the tyrosine kinase FGF receptors (FGFRs), leading to receptor activation and biological response.[14] Whereas binding to FGF2 essentially involves only two sulfate groups (the NSO_3 of a GlcN residue and the OSO_3 of an $IdoA2SO_3$ residue) of a disaccharide unit of heparin, formation of ternary complexes with FGFs and FGFRs requires several pairs of these groups (as well as some 6-*O*-sulfate groups) along heparin chains longer than 8−10 monosaccharide units.[14,15] Reported strategies to develop antiangiogenic agents based on competition with HSPGs for binding FGF2 while preventing formation of FGF2/FGFR complexes involve use of small heparin oligosaccharides[16] or removal of heparin 6-*O*-sulfate groups necessary for activation of the FGF2−FGFR complexes.[17]

Our novel strategy for designing heparin-like FGF2 inhibitors with potential antiangiogenic activity was based on generation of regular sulfation gaps along the NS regions of heparin chains, followed by glycol-splitting of all nonsulfated uronic acid residues. These modifications were performed by a modulated basic treatment of heparin, leading to selective removal of 2-*O*-sulfate groups with formation of epoxide derivatives, followed by hydrolysis of the epoxide rings[18−20] and periodate oxidation/borohydride reduction[21] of the resulting L-GalA residues as well as the preexisting nonsulfated GlcA and IdoA residues. We recently reported[22] that a prototype derivative (where about 50% of the total uronic acid residues were glycol-split) prevents the formation of HSPG/FGF2/FGFR ternary complexes in a FGF2-mediated cell−cell adhesion assay as efficiently as heparin. It also partially prevented FGF2 dimerization and inhibited FGF2-induced endothelial cell proliferation. Finally, it exerted a significant antiangiogenic activity in a chick embryo chorioallantoic membrane (CAM) model in which unmodified heparin is inactive.[22] Herein we report a systematic study of the effects of graded removal of 2-*O*-sulfate groups and controlled glycol splitting on the in vitro FGF2-antagonist activity (evaluated as inhibition of the formation of the HSPG/FGF2/FGFR ternary complexes and endothelial cell growth) and in vivo angiostatic activity in the CAM assay of a series of heparin derivatives. Our results support the concept that 2-*O*-desulfation and further chemical modification of a number of $IdoA2SO_3$ residues along the heparin chains inhibit activation of the growth factor and confer a potent antiangiogenic activity to heparin-derived compounds. In combination with molecular modeling calculations, they also confirm that glycol-split residues act as flexible joints along the polysaccharide chains and induce molecular conformations unfavorable for the formation of ternary complexes with FGF2 and FGFR.

Results

Synthesis and Structural Characterization of Modified Heparins. The strategy used in the present work for chemical modification of heparin (**1**) is schematized in Figure 1. Sulfate groups at position 2 of the IdoA residues of heparin have been removed under controlled basic conditions in a way to permit graded 2-*O*-desulfation through formation of intermediate epoxides (step a), followed by opening of the epoxide rings (step b) to afford L-GalA derivatives.[18−20] (See Experimental Section). Through this route reactions could be better controlled to afford heparin derivatives with degrees of conversion to GalA residues ranging from 14% to 42% of the original content of $IdoA2SO_3$ residues. Epoxides **2**−**4** (H-[14]e, H-[24]e, and H-[30]e) and the GalA

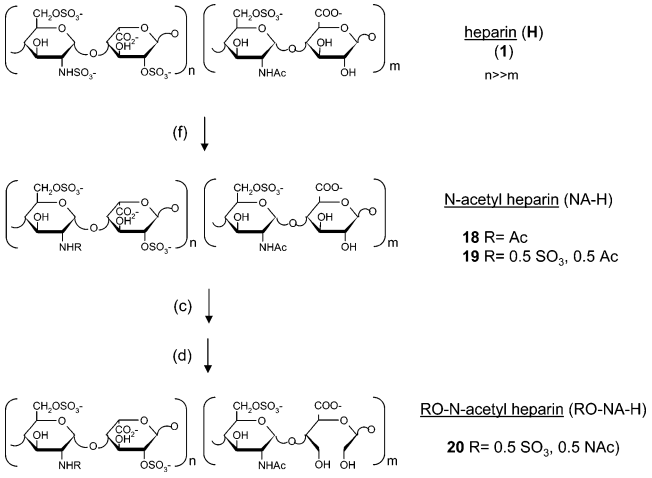

Figure 2. *N*-Acetylation of heparin (step f) and glycol splitting/reduction of *N*-acetyl heparins (steps c and d).

derivatives **5**−**7** (H-^{14}GalA, H-^{24}GalA, and H-^{42}GalA), where superscripts refer to the percent conversion of IdoA2SO_3 to epoxide or GalA, have been isolated and their structure characterized by ^{1}H and ^{13}C NMR spectroscopy. Quantification of epoxidated and GalA residues groups was based on typical ^{13}C signals at 53.5/54.5 ppm. GalA residues were determined indirectly by monitoring the disappearance of the epoxide signals. All nonsulfated uronic acid residues have been subsequently oxidized with periodate (step c) and either reduced with borohydride (step d, leading to H-gs **8**−**15**) or converted to glycine and taurine derivatives (step e, products H-gs/G (**16**) and H-gs/T (**17**)). The glycol-split low molecular weight and very low molecular weight derivatives **14** and **15** were prepared by controlled nitrous acid depolymerization of glycol-split heparins as described in the Experimental Section. The degree of glycol splitting was determined by ^{13}C NMR (signal at 106.5 ppm).[22] Heparin was also periodate oxidized/borohydride reduced without prior 2-*O*-desulfation, to obtain "reduced oxyheparin" (RO−H, here designated H-^{25}gs, **8**). In this reference compound, glycol splitting occurred only at the level of preexisting nonsulfated GlcA and IdoA residues, which corresponds to about 25% of total uronic acids of the parent heparin **1**. Also as reference compounds, *N*-acetylated heparins NA-H (**18**) and ^{50}NA-H (**19**) (where all and ∼50% N−SO_3 groups, respectively, were replaced by *N*-acetyl groups) as well as the periodate oxidized/borohydride reduced derivative of the latter ^{50}NA-H-^{25}gs, **20**) were prepared (Figure 2). All products gave a single (broad but symmetrical) GPC−HPLC peak and migrated as a single electrophoretic band. The average molecular weights (MW), the corresponding polydispersity (Pd), and the degrees of sulfation (DS) of all products are reported in Table 1. Whereas the 2-*O*-desulfation reactions (epoxide ring formation and opening with formation of L-GalA derivatives) did not significantly modify the molecular size of the parent heparin (15 800 Da), the MW values of glycol-split derivatives are somewhat lower (11 600−13 800 vs 13 100−18 800). Molecular weights of derivatives of heparin **1** are somewhat more polydispersed than the parent compound (Pd 1.2−1.4 vs 1.1), with a larger spreading observed for the epoxide derivatives. The low and very low molecular weight derivatives showed the highest molecular weight dispersions: 1.4 for **14** (LMW-H-^{52}gs) and 2.2 for **15** (vLMW-H-^{52}gs) (Table 1).

Table 1. Average Molecular Weight (MW), Polydispersion (Pd),[41] Sulfation Degree (DS),[42] Inhibition of FGF2-mediated Cell−Cell Adhesion[25] and Endothelial Cell Proliferation,[25] and Antiangiogenic Activity in CAM Assay[26] for Heparin and Heparin Derivatives[a]

					(ID_{50}, ng/mL)		
no.		MW	Pd	DS	cell−cell adhesn	cell prolif	% inhibn (CAM)[b]
1	heparin	15800	1.1	2.2	100	2000	<30
	2-*O*-Desulfated Heparins						
2	H-^{14}e	17600	1.3	2.0	10	300	nd
3	H-^{24}e	17800	1.4	2.0	30	2000	nd
4	H-^{30}e	18800	1.4	1.9	100	1000	nd
5	H-^{14}GalA	13100	1.2	2.0	500	30000	nd
6	H-^{24}GalA	12900	1.2	2.0	70	300	30
7	H-^{42}GalA	13200	1.2	1.8	300	1000	nd
	Glycol-Split Heparins						
8	H-^{25}gs	11600	1.2	2.2	1 000	3000	30
9	H-^{33}gs	11900	1.2	2.1	100	3000	40
10	H-^{42}gs	11700	1.2	2.0	100	1000	40
11	H-^{46}gs	11900	1.2	1.7	100	300	80
12	H-^{58}gs	13800	1.2	1.6	30	100	80
13	H-^{74}gs	12800	1.3	1.5	10	100	60
14	LMW-H-^{52}gs	5800	1.4	1.7	30	300	70
15	vLMW-H-^{52}gs	3000	2.2	1.7	30	300	90
	Derivatives of Glycol-Split Heparins						
16	H-^{74}gs/G	nd[c]	nd	nd	10	3000	80
17	H-^{74}gs/T	nd	nd	nd	300	1000	70
	N-Acetylated Heparins						
18	^{100}NA-H	11300	1.3	1.5	30000	>100000	<30
19	^{50}NA-H	10900	1.3	1.8	3000	1000	<30
20	^{50}NA-H-^{25}gs	12100	1.3	1.7	300	30000	30

[a] Percent conversions are indicated as superscripts on symbols of products. [b] 100 μg/embryo. [c] nd: not determined.

The structure of products was determined mainly by one- and two-dimensional ^{1}H and ^{13}C NMR spectroscopy.[22,23] Product **12** (H-^{58}gs, obtained upon ∼58% glycol splitting of total uronic acid residues) was characterized in some more detail. The ^{1}H and ^{13}C NMR spectra of **12** have been already reported[22] and indicate that the structure of the products is prevalently represented as shown in Figure 3. This structure was further confirmed by NMR spectroscopic and MALDI mass spectrometric analysis of the fragments obtained by Smith degradation[24] of **12**. Fragments prevalently consisted of the trisaccharide GlcN$SO_3$6SO_3−IdoA2SO_3−GlcN$SO_3$6SO_3−R, where R is the remnant of a glycol-split uronic acid residue cleaved under the mild acid conditions of the Smith degradation (i.e., D-threonic acid when derived from L-IdoA or L-GalA). To evaluate the molecular weight dependence of biological activities of undersulfated, glycol-split heparins, low molecular weight and a very low molecular weight derivatives of prototype **12** (**14**, LMWH-^{52}gs; **15**, vLMW-H-^{52}gs) were prepared by nitrous acid depolymerization/borohydride reduction of 52% glycol-split heparins (see Experimental Section). The chains of these derivatives terminate at the reducing end with a residue of 2,5-anhydromannitol. 2D NMR analysis (see Experimental Section) indicates that this residue is linked to an unmodified IdoA2SO_3 residue as shown in Figure 3, with no evidence for the alternative bond to a glycol-split L-GalA residue. To evaluate the effect of substituents at the level of glycol split residues, the 74% glycol-split heparin derivative **13** was converted

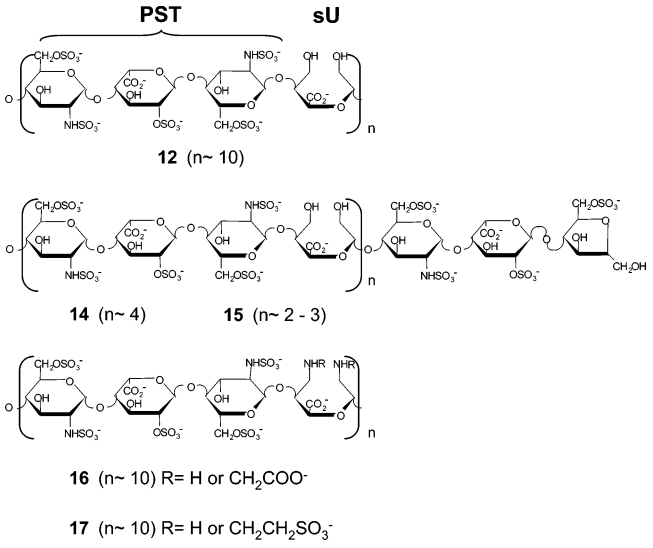

Figure 3. Prevalent structures of **12**, a product obtained by glycol-splitting/reduction of L-GalA analogues of heparin; **14** and **15**, LMW and vLMW derivatives; **16** and **17**, glycine and taurine derivatives. **12** was obtained under conditions to modify approximately 50% of the original 2-*O*-sulfated iduronic acid residues in the NS regions of heparin)[22] and it is constituted by pentasulfated trisaccharide (PST) sequences separated from each other by glycol-split uronic acid residues (sU). LMW and vLMW derivatives **14** and **15** were obtained from a glycol-split LMW heparin and terminate with 2,5-anhydromannitol residues. The glycine and taurine substitution in **16** and **17** were 48% and 69%, respectively. (See the text.)

into its glycine and taurine derivatives (**16**, H-^{74}gs/G; **17**, H-^{74}gs/T). The prevalent structures of these products are shown in Figure 3.

FGF2-Antagonist, Antiangiogenic Activities. Heparin derivatives were assessed for their FGF2 antagonist and antiangiogenic activity in vitro (disruption of the FGFR/FGF2/HSPG ternary complex in a FGF2-mediated cell−cell adhesion assay and inhibition of FGF2-mediated endothelial cell proliferation) and in vivo (inhibition of neovascularization in the chick embryo CAM assay) (Table 1).

In the FGF2-mediated cell−cell adhesion test, FGF2 causes cell−cell attachment by linking FGFRs carried on FGFR1-overexpressing HSPG-deficient CHO mutants to HSPGs expressed by neighboring wild-type CHO-K1 cells.[25] In this assay, several of the present heparin derivatives prevent the formation of the FGFR/FGF2/HSPG ternary complex with a potency similar to or better than that shown by heparin (ID_{50} = 100 ng/mL). Compounds with the highest activity (ID_{50} = 10−30 ng/mL) are the epoxides **2** (H-^{14}e) and **3** (H-^{24}e) and the glycol-split derivatives **12** (H-^{58}gs), **13** (H-^{74}gs), as well as the low molecular weight and very low molecular weight derivatives **14** (LMW-H-^{52}gs) and **15** (vLMW-H-^{52}gs) and the glycine derivative **16** (H-^{74}gs/G).

In the endothelial cell proliferation assay,[25] the most potent FGF2 antagonists (ID_{50} = 100 ng/mL) are **12** (H-^{58}gs) and **13** (H-^{74}gs), whereas heparin (**1**) is poorly effective (ID_{50} = 2000 ng/mL). Also active in this test are **2** (H-^{14}e), **6** (H-^{24}GalA), **11** (H-^{46}gs), **14** (LMW-H-^{52}gs), and **15** (vLMW-H-^{52}gs) (ID_{50} = 100−300 ng/mL).

In the CAM assay,[26] where heparin is inactive, most of the tested products exert an antiangiogenic effect in vivo. Highest activities (inhibition of 60−90%) were observed for heparins glycol-split to extents higher than 45% and for their derivatives. Indeed, the very low MW derivative **15** showed the highest activity in the series. The negative control *N*-acetyl heparin (**18**,^{100}NA-H) was essentially inactive in all the tests. However, a weak inhibition of FGF2-mediated cell−cell adhesion and endothelial cell proliferation was observed with **19** (^{50}NA-H, where only about half of the GlcN residues of heparin are *N*-sulfated). The glycol-split variant of **19** (**20**,^{50}NA-H-^{25}gs) showed some minor activity in the CAM assay.

As illustrated in Figure 4A, the capacity of each compound to prevent the formation of the FGFR/FGF2/HSPG ternary complex in the FGF2-mediated cell−cell adhesion assay is significantly related to its FGF2-

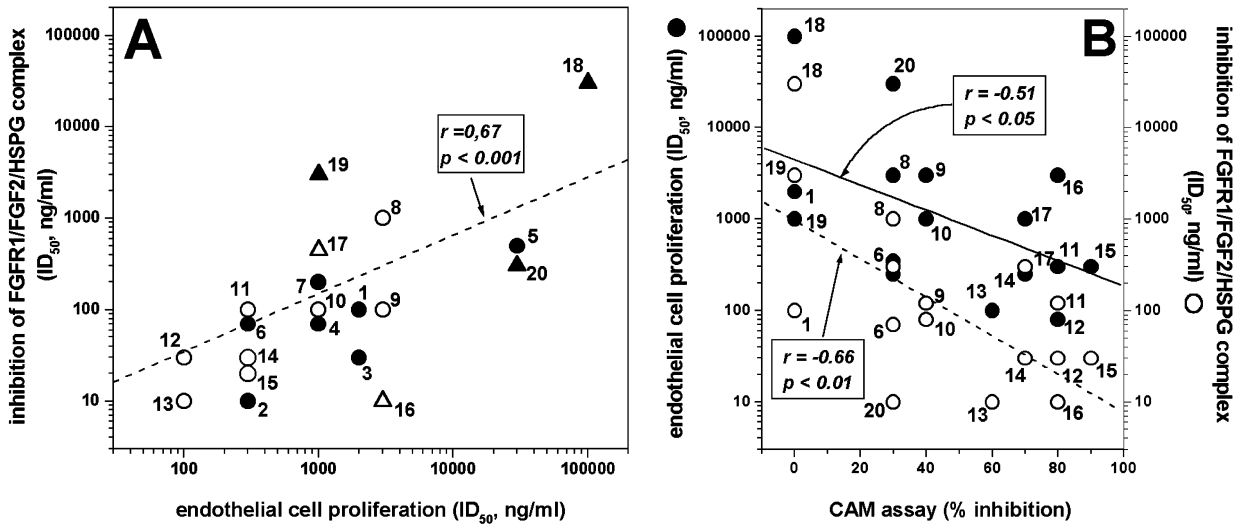

Figure 4. FGF2-antagonist, antiangiogenic activities of heparin derivatives. (A) The inhibitory potencies (expressed as ID_{50}, ng/mL) in the endothelial cell proliferation assay and in the FGF2-mediated cell−cell adhesion assay are plotted for each compound. A significant relationship is observed between the two FGF2-antagonist activities. ●, heparin and 2-*O*-desulfated heparins; ○, glycol-split heparins; △, glycol-split heparin derivatives; ▲, *N*-acetylated heparins. (B) The potencies of heparin derivatives in the endothelial cell proliferation assay (●) and in the FGF2-mediated cell−cell adhesion assay (○) are significantly related to their antiangiogenic activity in the CAM assay.

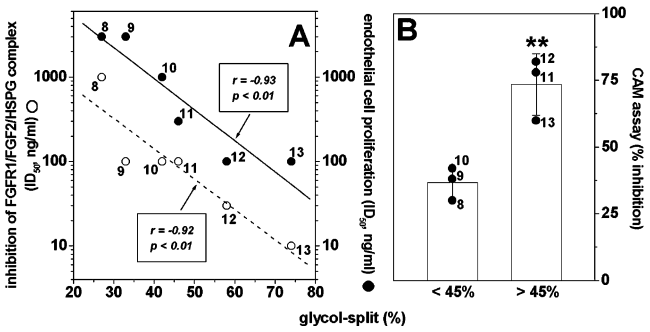

Figure 5. Effect of glycol-splitting on the FGF2-antagonist, antiangiogenic activities of heparin derivatives. (A) The potencies of glycol-split heparins in the endothelial cell proliferation assay (●) and in the FGF2-mediated cell−cell adhesion assay (○) are significantly related to their degree of glycol-splitting. (B) Compounds with extensive glycol splitting (>45%) show a significantly higher angiostatic activity when compared to compounds with glycol splitting lower than 45% (**, $p > 0.01$).

antagonist activity in the endothelial cell proliferation assay, confirming that both assays reflect the FGF2-binding capacity of the compound. Interestingly, the results obtained in both the in vitro tests significantly relate with those obtained in the in vivo CAM assay (Figure 4B), where neovascularization is strongly dependent on the activity of endogenous FGF2 produced by the chick embryo.[27] Also, a significant correlation exists between the potency shown by the various glycol-split heparins in the two in vitro assays and their degree of splitting (Figure 5A), indicating that the FGF2-antagonist activity of these derivatives increases upon increasing the number of glycol-split uronic acid residues along the heparin chain. A similar significant trend is also observed for inhibition of angiogenesis in the CAM assay, with derivatives with a degree of glycol-splitting higher than 45% showing a significantly higher angiostatic effect (Figure 5B).

Molecular Conformation and Dynamics. To investigate whether conformational properties induced by glycol splitting in the heparin sequences could influence binding to FGF2 and account for the observed induction of FGF2-antagonist properties, advantage was taken of the availability of X-ray diffraction data of the heparin hexasaccharide $\Delta U2SO_3-GlcNSO_36SO_3-IdoA2SO_3-GlcNSO_36SO_3-IdoA2SO_3-GlcNSO_36SO_3$ (H-Hexa) cocrystallized with FGF2 (Protein Data Bank Code 1BFC).[28] The corresponding glycol-split hexasaccharide $\Delta U2SO_3-GlcNSO_36SO_3-IdoA2SO_3-GlcNSO_36SO_3-$gs-GalA−$GlcNSO_36SO3$ (sU-Hexa), created using Macromodel version 7.1, was modeled in the presence of FGF2, and its 3D structure was compared with that of H-Hexa in its complex with the growth factor. On the basis of crystallographic data,[29] the I2A2 disaccharide moieties of both H-Hexa and sU-Hexa were locked to the protein binding site by constraints described in the Experimental Section. The conformational freedom of the rest of the molecule was explored by Monte Carlo/stochastic dynamics (MC/SD). This method combines the ability of SD to efficiently explore a local low-energy area with the capacity of MC to interconvert conformations separated by large energy barriers.[28,30] MC/SD gave preliminary information on the different ability of freely moving moieties of the two molecules to explore their conformational space. Interglycosidic torsional angles φ and ψ of A2-sU and sU-A3 linkages were monitored during MC/SD calculation, in comparison with the corresponding torsions of H-Hexa (Figure 6). During MC/SD, both sU-Hexa and H-Hexa explored just one low-energy area located at φ,ψ (−60°→ 30°, −30°→ 60°) and φ,ψ (−90°→ −30°, −90°→ −30°), respectively. Torsional angles showed a larger dispersion (especially as regards ψ) in sU-Hexa than in H-Hexa, as also observed in sU-Hexa for the glycosidic linkage sU-A3 between the glycol-split residue and the following amino sugar residue. During dynamics, this linkage of the glycol-split hexasaccharide explored two low-energy areas, one of which (corresponding to the area found for H-Hexa) was located at φ,ψ (−20°→ 80°, −60°→ 60°) and the other located at φ,ψ (−90°→ 0°, −90°→ 0°). During MC/SD of sU-hexa, also the conformation of the glycol-split residue sU3 assumed two different geometries, characterized by a C5−O5−C1−H1 torsion angle swinging around 180° and 0°, respectively. Only the first of these values is similar to C5−O5−C1−H1 observed for the $IdoA2SO_3$ residue in H-Hexa. In both cases, also this torsion presents a considerably broad distribution (data not shown). It is important to note that for almost all the structures having C5−O5−C1−H1 torsion angles near to 180°, during MC/SD the sU-A3 glycosidic linkage geometry explored the φ,ψ area (−20°→ 80°,

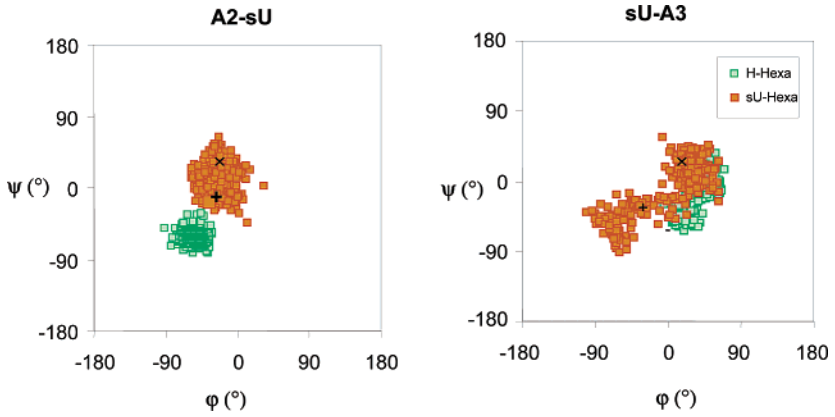

Figure 6. Scatter plots of φ and ψ torsional angles for A2-sU and sU-A3 glycosidic linkages of the glycol-split hexasaccharide (sU-Hexa, orange squares) and the heparin hexasaccharide (H-Hexa, green squares), designated as A1-I1-A2-I2-A3-I3 and A1-I1-A2-sU-A3-I3, respectively, where A is $GlcNSO_36SO_3$, I is $IdoA2SO_3$, and sU is a glycol-split GalA residue. Minima distribution was obtained by MC/SD calculation. SU-Hexa structures with the largest (+) and smallest (×) A3-NS···ϵN-Lys27 distance are shown.

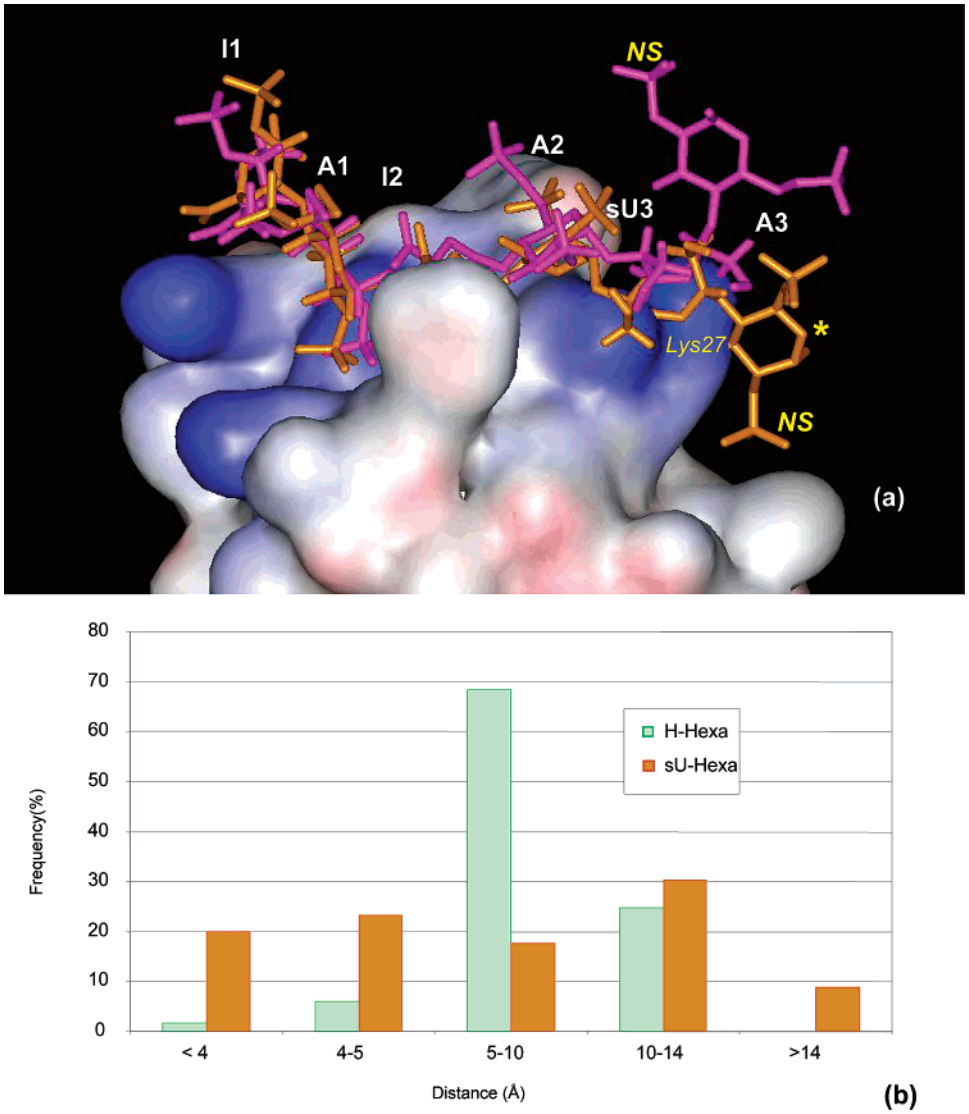

Figure 7. (a) FGF2 hexasaccharide complexes: glycol-split hexasaccharide (sU-Hexa) conformers with the largest (violet) and smallest (orange) A3-NS···ϵN-Lys27 distance obtained by MCSD calculation. A1-NS and I2-2S groups were locked into the protein binding site. The asterix indicates the position of S in the A3-NS group of H-Hexa complexed with FGF2 from X-ray structure (4.4 Å from ϵN-Lys27).[27] (b) Comparison between A3-NS···ϵN-Lys27 distance frequency observed during MCSD simulation in su-Hexa and H-Hexa.

−60°→ 60°), whereas for structures having the above torsion angle near to 0° it essentially explored the φ,ψ area (−90°→ 0°, −90°→ 0°).

To understand how this higher flexibility affects protein−ligand interactions, geometries found during MC/SD calculations for sU-Hexa were compared with those[29] found for H-Hexa cocrystallized with FGF2. In some of these geometries the reducing end of the glycol-split hexasaccharide is spread out from FGF2, whereas in others it is closer to the protein surface (Figure 7a). Taking into account A3−NS···ϵN−Lys27 as reference distance, it can be noted that this fluctuation is consistently larger and more evenly distributed in sU-Hexa than in H-Hexa (Figure 7b).

Discussion

Heparin behaves as a proangiogenic substance in biological models in which neovascularization is promoted by FGF2.[12] It is generally agreed that heparin/HS chains activate the growth factor by stabilizing ternary complexes with FGF2 and FGFRs.[3,4] Though with somewhat different geometries depending on the system, several X-ray diffraction studies have shown that such a stabilization occurs through settling of the heparin chains into "basic canyons" formed by alternate FGF and FGFR molecules.[31,32] A wealth of biochemical evidence indicates that formation of ternary complexes requires heparin chains longer than 6−8 saccharides.[15,16] On the basis of the assumption that even longer heparin chains could lose their ternary-complex-stabilizing property when the arrays of sulfate groups involved in the interaction with FGFs and FGFRs are interrupted by sulfation gaps, we synthesized in a previous work a prototype heparin derivative in which one sulfate group out of two IdoA2SO_3 residues in the regular (NS) region was removed. Then we further marked the interruption between the unmodified sequences by glycol splitting the nonsulfated uronic acid residues.[22] Such a prototype (product **12** of the present work) displaces the growth factor from its ternary complex with HSPG and FGFR1 as efficiently as heparin. However, it does not favor dimerization of FGF2,

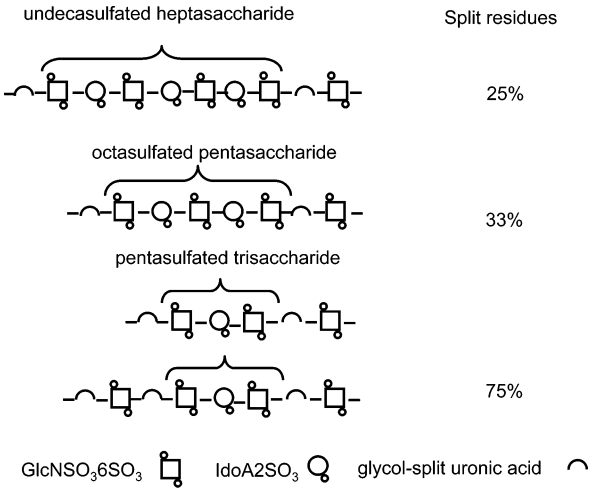

Figure 8. Schematic representation of regularly sulfated heparin sequences separated by glycol-split uronic acid residues, obtained by controlled 2-*O*-desulfation/glycol splitting. Modification of one-fourth of $IdoA2SO_3$ residues in the NS region chiefly affords sequences of undecasulfated heptasaccharides; modification of one-third and one-half or more of these residues generates shorter regularly sulfated sequences (octasulfated pentasaccharides and pentasulfated trisaccharide, respectively). (See the text.)

it inhibits FGF2-stimulated proliferation of endothelial cells, and it showed angiostatic activity in a CAM assay in which unmodified heparin is inactive.[22] In this work, the influence of controlled 2-*O*-desulfation/glycol splitting of heparin on structural and FGF2-associated biological properties has been more systematically studied.

At least a limited number of 2-*O*-sulfate groups are needed for significant binding of heparins to FGF2.[10] Some of the present undersulfated heparins retain the FGF2-binding capacity of the parent heparin, as estimated from their capability to prevent the formation of the FGFR/FGF2/HSPG ternary complex in a FGF2-mediated cell−cell adhesion test. Binding to FGF2 is thought a prerequisite for a molecule to act either as inhibitor or activator of the growth factor. The observed inhibition of FGF2-induced proliferation of endothelial cells and of neovascularization in the CAM model suggests that binding to FGF2 can be exploited to generate FGF2 inhibitors. A clear indication was also provided by the observation that inhibitory activities are systematically amplified by glycol splitting of the newly formed nonsulfated GalA residues, as well as of the preexisting nonsulfated uronic acids (GlcA and IdoA). The present work also indicates that the potent antiangiogenic properties of heparins that are 2-*O*-desulfated/glycol-split to the extent of more than 45% of total uronic acid residues as in derivative **12** are retained even by low and very low MW derivatives **14** and **15**, with approximately the same degree of splitting as **12**. The shortest investigated chain corresponds to two or three repeating sequences of the pentasulfated trisaccharide PST (Figure 3). Moreover, also substitution at the level of glycol-split residues (such as for the glycine and taurine derivatives **16** and **17**) does not impair the antiangiogenic activity measured in the CAM model.

The idealized sequences of Figure 8 illustrate the prevalent structures obtained for different degrees of 2-*O*-desulfation/glycol splitting in the NS region of heparin. The glycol-split residues interrupt regular, homogeneously sulfated sequences of different length depending on the extent of splitting. Whereas splitting of one out of four uronic acid residues "frames" heptasaccharidic sequences, splitting of one out of three or out of two residues results in pentasaccharidic and trisaccharidic sequences between glycol-split residues, respectively. Some trisaccharidic sequences separated by glycol-split residues are also retained in more extensively 2-*O*-desulfated/glycol-split heparin chains, as in the ∼75% modified derivative. Since the most extensively glycol-split heparin in the present work (**13**, H-^{74}gs) has the highest activity in the in vitro assays (along with a significant angiostatic activity in vivo) as compared with its less modified homologue **12** (H-^{58}gs), it can be inferred that very few PST sequences along a heparin chain are sufficient to induce significant angiostatic properties, provided these sequences are separated from each other by sequences containing one or more sU residues.

The concept that glycol-split residues act as flexible joints along the GAG chains, thus facilitating docking of active sequences to target proteins,[33] is strongly supported by the present study. Glycol splitting of naturally occurring, nonsulfated uronic acids of heparin has been reported to potentiate activities associated with interactions involving sequences within the NS region of the GAG, such as binding with lipoproteinlipase.[21] heparin-cofactor-2,[21] and heparanase.[34] Glycol-split residues appear to exert this function also in the interaction with FGF2 (and probably also with other growth factors). Preliminary NMR and molecular modeling studies on prototype **12** (whose PST sequences contain the minimal FGF2-binding disaccharide sequence $GlcNSO_3$−$IdoA2SO_3$) suggested that glycol splitting induces a drastic divergence of the GAG chain from the linear propagation required for settling in the basic canyon generated by FGF/FGFR assemblies, thus providing a clue to explain the antiantiogenic activity of the product.[22] The present molecular dynamics data further support the concept that glycol-split heparin chains are consistently more flexible than unmodified chains and conformationally driven to adopt geometries unfavorable for formation of ternary complexes with FGF2 and its receptor(s). Further SD simulations are in progress to study in greater detail the time evolution of unmodified and glycol-split hexasaccharides in their complex with FGF2. The present results also confirm the original assumption[22] that controlled generation of sulfation gaps along the heparin chains followed by glycol-splitting of the newly formed nonsulfated uronic acids (in this case, GalA) does not impair the ability of heparin to form 1:1 complexes with FGF2, but conceivably makes formation of active complexes with FGFR very unfavorable. Indeed, as illustrated in Figure 7, the present molecular dynamics calculations indicate that—at least at the hexasaccharide level—some conformers of glycol-split chains may favor 1:1 complexes with FGF2 also through interaction of their sulfamino group A3-NS with Lys27 of the protein. It is still not yet clear whether the presence of more than one PST sequence in chains containing glycol-split residues enhances the angiostatic ability (conceivably, by a "multivalence

effect") or if the same activity could be achieved by the same molar equivalents of a PST trisaccharide. It must be noted that most of the products with degrees of splitting corresponding to lower or higher than 50% modification of total uronic acids of heparin have hybrid structures containing more than one of the sequence types depicted in Figure 8. Even the remarkable cleanliness of the one- and two-dimensional NMR spectra of the prototype of this series, clearly supporting its prevalent structure **12**,[22] conceals some structural heterogeneities common in GAGs and their derivatives. As mentioned in the Results, the Smith degradation analysis of **12** confirmed the trisaccharide PST.R as a major fragment, but also revealed the corresponding pentasaccharide as a minor one.

No attempts were made to detect in our heparin derivatives the presence of $GlcNSO_3$,3,$6SO_3$ residues that are typical components of the pentasaccharide sequences of the active site for antithrombin. This sequence is contained in only about one-third of the heparin chains as part of the NS regions.[10] It is accordingly expected that some of the sequences framed between glycol-split residues occasionally contain an extra 3-*O*-sulfated glucosamine. However, 3-*O*-sulfate groups were shown to be removed under conditions of alkali-induced 2-*O*-desulfation.[35] A further, dramatic loss of anticoagulant activity is expected upon glycol splitting of the essential GlcA residue of the antithrombin-binding sequence.[21,36] Indeed, the present heparin derivatives have a very low anticoagulant activity.[37]

In conclusion, a novel family of nonanticoagulant heparin derivatives is described, some of which retain the FGF2-binding properties of heparin but are antiangiogenic in a CAM model in which heparin is inactive. Current studies on two prototypes and their LMW derivatives are indicating that they inhibit also the activity exerted in vitro by the angiogenic heparin-binding $VEGF_{165}$ isoform, are antiangiogenic in a number of in vivo tests, and are antimetastatic in experimental animal models.[37]

Experimental Section

All solvents and reagents were of analytical grade and were used as received. Heparin (H, **1**) was a preparation of porcine mucosal heparin sodium salt (170 IU/mg, FU IX) from L.D.O., Trino Vercellese, Italy; its purity was assessed by NMR analysis.[23] Human recombinant FGF2 was purified from *Escherichia coli* cell extract by heparin-Sepharose affinity chromatography.[38] Desalting of heparin derivatives was carried out by dialysis against water through 1000 Da cutoff tubes (Thomas) or by fractionation on a 2.5 × 100 cm Sephadex G10 (Pharmacia) column, with 10% EtOH in water as eluent and UV detection at 210 nm. Assessment of homogeneity of products was made by HPLC[39] and by cellulose acetate electrophoresis in HCl buffer.[40] Molecular weight analysis, with determination of average molecular weights (MW) and polydispersion (Pd), were made by GPC−HPLC using the triple detector technology,[41] on a Viscotex instrument equipped with a VE112 pump, 100 μL injector loop, and TDA302 detector provided with refractive index, viscosimeter, and 90° light scattering systems. Eluent was 0.1 M $NaNO_3$ (flow 0.6 mL/min). Samples were dissolved in the eluent solution (15 mg/mL). The degree of sulfation (DS) was determined by conductometric titration of samples in the acid form,[42] using a Mettler DL40GP memotitrator and an Amel 160 conductimeter.

The 1D homo and 2D NMR spectra were obtained at 500 MHz for ^{1}H with a Bruker Avance 500 spectrometer, equipped with a 5-mm TXI probe, from D_2O solutions (15 mg/0.5 mL of D_2O, 99.99% D) or, for long experiments, from buffer solutions (10 mM phosphate buffer pH 7 in D_2O). ^{13}C 1D NMR spectra were obtained at 100 MHz for ^{13}C, with a Bruker AMX400 spectrometer, equipped with a multinuclear 10-mm probe, from D_2O solutions (50−100 mg/mL). Chemical shifts, given in parts per million downfield from sodium-3-(trimethylsilyl)-propionate, were measured indirectly with reference to acetone in D_2O (δ 2.235 for ^{1}H and δ 33.08 for ^{13}C). The spectra were recorded at 45 °C. The ^{1}H, COSY, and TOCSY spectra were obtained with presaturation of the HOD signal. Sulfation patterns (percent distribution of sulfate groups in different positions of the IdoA and GlcN residues and percent *N*-sulfation of GlcN residues) were detected by quantification of ^{13}C signals as described.[23] Percent conversion (to epoxide derivatives, GalA derivatives, and glycol-split derivatives, indicated as superscripts on product symbols) was based on integration of typical ^{13}C signals and comparison of their area to those of total anomeric signals as indicated below for the three series of products. Whenever checked for different preparations of the same derivative, conversion degrees were reproducible (±1%). MALDI mass spectrometric analysis of oligosaccharidic products was carried out in positive mode on a Bruker Biflex III time-of-flight instrument equipped with a pulsed nitrogen laser (337 nm) using the basic peptide $(Arg\text{-}Gly)_{19}Arg$ as previously described.[43]

Epoxy Heparins (H-e). 2,3-Epoxidation through selective *O*-desulfation at C2 of the IdoA residues was performed by alkaline treatment of heparin following a modification of the method of Piani et al.[20] **1** (1 g) was dissolved in 6.25 mL of water, then 6.25 mL of 2 M NaOH was added and the mixture stirred at 60 °C for different times in order to obtain different products (15 min for H-^{14}e (**2**), 30 min for H-^{24}e (**3**), and 45 min for H-^{30}e (**4**). After cooling below 30 °C, the solution was brought to pH 7 with 0.1 M HCl, then desalted by dialysis, and freeze-dried. The resulting heparin epoxides (**2**−**4**, as Na salts) were obtained in 78%, 74%, and 80% yields, respectively. The degree of epoxidation (de, expressed as molar ratios of epoxidated rings to total uronic acids) was evaluated by ^{13}C NMR spectroscopy from the area of the C2 and C3 signals of the 2,3-anhydropyranose residue at 53.5/54.5 ppm (*A*) and that of total anomeric signals at 98−104 ppm (*B*) and calculated as follows: $de = A/B \times 100$.

Galacturonic Acid Analogues of Heparin (H-GalA). Conversion of epoxide derivatives to L-GalA analogues was performed by modification of published methods,[18−20] either starting from a previously isolated intermediate epoxide or directly from heparin. Aqueous solvolysis of epoxides **2** and **3** (400 mg, in 10 mL, at 70 °C for 48 h after cooling below 30 °C, dialysis, and freeze-drying) gave H-^{14}GalA (**5**) and H-^{24}GalA (**6**) in 91% and 79% yields, respectively. The 42% converted product H-^{42}GalA (**7**) was obtained starting directly from heparin. **1** (1 g) was dissolved in 6.25 mL of water, stirred at 60 °C, then 6.25 mL of 2 M NaOH was added. After 1 h of stirring at 60 °C and cooling at 30 °C, the solution was brought to pH 7 with 0.1 M HCl and then heated for 24 h at 70 °C. After cooling and desalting, product **7** was isolated by freeze-drying in an overall yield of 57%. Reactions were monitored by ^{13}C NMR and kept going up to complete disappearance of the epoxide signals at 53.5/54.5 ppm, with the corresponding emergence of the GalA C-1 peak at 102.0 ppm. Percent conversions to GalA analogues (indicated as suffixes in product symbols) were accordingly assumed to be the same as determined for the intermediate epoxide derivatives.

Glycol-Split Heparins (H-gs). Heparin and GalA analogues of heparin were exhaustively periodate oxidized/borohydride reduced as described for unmodified heparin,[21] starting from **1** to obtain H-^{24}gs (**8**) and from GalA analogues of different degrees of conversion to obtain the other glycol-split heparins (**9**, H-^{33}gs; **10**, H-^{42}gs; **11**, H-^{46}gs; **12**, H-^{58}gs; **13**, H-^{75}-gs, where superscripts indicate the degrees of glycol-splitting of total uronic acid residues, i.e., GalA + GlcA + IdoA). The corresponding intermediate GalA analogues were **5** for **9**, **6** for **12**, and **7** for **13**. The GalA intermediates for **10** and **11** were isolated only in amounts sufficient for ^{13}C NMR analysis.

1 or H−GalA (1 g) of different degrees of conversion were dissolved in 25 mL of water and to the solution was added 25 mL of 0.1 M $NaIO_4$ solution. The solution was stirred at 4 °C for 16 h in the dark. The reaction was stopped by adding 5 mL of diethylene glycol and the solution was dialyzed for 16 h. Solid sodium borohyride (250 mg) was added to the retentate solution in several portions under stirring. After 2−3 h the pH was adjusted to 3 with 0.1 M HCl, and the solution was neutralized with NaOH. After dialysis, the final product was recovered by freeze-drying. The percent glycol splitting (gs) was calculated by ^{13}C NMR from the area of the anomeric signal of glycol-split uronic acids (at 106.5 ppm, *A*)[22] and the area of the anomeric signal of 2-*O*-sulfated iduronic acids (at 102.0 ppm, *B*); gs = $A/A + B \times 100$. Yields for **8**−**13** = 80−90%.

Low Molecular Weight and Very Low Molecular Weight Glycol-Split Heparins. LMW-H-^{52}gs (**14**) and vLMW-H-^{52}gs (**15**) were prepared by controlled nitrous acid depolymerization[44] of the appropriate glycol-split heparin. For **14**, 4 g of H-^{52}gs (prepared as described above for slighly different degrees of conversion) was dissolved in 65 mL of H_2O at 4 °C, 75 mg of $NaNO_2$ was added, and the pH was adjusted to 2 with 0.1 M HCl. The solution was stirred at 4 °C for 20 min. The pH was then brought to 7. Solid $NaBH_4$ (1 g) was added in several portions under stirring. After 2−3 h the pH was adjusted to 4 with HCl, then the solution was neutralized with 0.1 M NaOH. The product was isolated by adding 3 vol of EtOH. The precipitate was solubilized in water and recovered by freeze-drying. The extent of glycol spliting was evaluated as described for H-gs. The depolymerization degree (*n*, as defined in Figure 2) was evaluated by integration of all anomeric ^{13}C NMR signals at 98−107 ppm (*A*) and those at 82, 85 and 87 ppm (*B*) corresponding to C2, C3, and C5 of the terminal anhydromannitol unit. Since the anomeric signals account for two carbons and the considered anhydromannitol signals for three carbons, $n = A/B \times 3/2$. VLMW-H-^{52}gs (**15**) was isolated in a 23% yield from crude **14** (before EtOH precipitation) by fractionation on a Sephadex G-25 column under conditions for desalting (150 × 2.5 cm, eluent 2 mL/min EtOH 10% in H_2O, collecting the highest retention time fraction).

Smith Degradation of Glycol-Split Heparin. The Smith degradation reaction (periodate oxidation, borohydride reduction, and mild acid hydrolysis)[24] was applied to H-^{58}gs (**12**) to cleave the glycosidic bonds of its glycol-split residues. **12** (1.2 g) was dissolved in 50 mL of 0.1 M HCl. The solution was stirred at 55 °C for 2 h and then cooled and neutralized with 0.1 M NaOH. The product was recovered by freeze-drying and fractionated by gel permeation chromatography (TSK.HW 40S). A major fraction was obtained, with a prominent MALDI-MS peak at *m*/*z* 1034.6 (calculated for trisaccharide 1034) and a minor peak at *m*/*z* 1611(calculated for pentasaccharide 1612.5).

Glycine and Taurine Derivatives of Glycol-Split Heparins. These derivatives were obtained by reductive amination[45] of polydialdehydes obtained by periodate oxidation of GalA analogues. Both derivatives were prepared from **7**, i.e., the GalA intermediate also used for preparation of **13**. To prepare the glycine derivative (**16**), **7** (300 mg) was dissolved in 7.5 mL of H_2O and then 7.5 mL of 0.2 M $NaIO_4$ solution was added. After stirring at 4 °C for 16 h in the dark, the reaction was stopped by adding 1 mL of ethylene glycol and the solution was dialyzed for 16 h. The solution volume (about 100 mL) was reduced to 12 mL under vacuum, then glycine (1.6 g) was added with stirring in several portions. After 1 h solid $NaBH_4$ (200 mg) was added in several portions under stirring and the pH was adjusted to 6 with 0.1 M HCl. After 3 h the pH was adjusted to 4 with 0.1 M HCl, and the solution was neutralized with 0.1 M NaOH. After desalting (which also removed unreacted glycine), the final product **16** was recovered in a 85% yield by freeze-drying. Typical ^{13}C NMR signals were 52 ppm ($NHCH_2CO_2$) and 106.5 ppm (C1 of glycol-split uronic acid residues). The extent of glycol-splitting (74%) was evaluated as described before for glycol-split heparins. The glycine molar substitution G% (48%, as referred to total split uronic acids) was evaluated from the area of ^{13}C NMR signals at 52 ppm (*A*) and 106.5 ppm (*B*), corresponding to CH_2 glycine signals and split uronic residues, respectively, as follows: G% = $A/B \times 100$. The taurine derivative **17** was prepared by following the same procedure described for **16**, using taurine instead of glycine (yield 57%). Typical ^{13}C NMR signals were 49.2 and 48.8 ppm (CH_2SO_3), 46.4 and 46.2 ppm ($NHCH_2$), and 106.5 ppm (C1 of glycol-split uronic acid residues). The taurine molar substitution T% (69%), as referred to total split uronic acids) was evaluated from the area of ^{13}C NMR signals at 49−46 ppm (*A*) and at 106.5 ppm (*B*), corresponding to CH_2 taurine signals and split uronic residues, respectively, as follows: G% = $A/B \times 100$.

***N*-Acetyl Heparins (NA-H).** Fully *N*-acetylated heparin (^{100}NA-H, **18**) was prepared from heparin as described.[46] Half *N*-acetyl heparin (^{50}NA-H, **19**) was prepared by solvolytic partial *N*-desulfation of heparin in DMSO/MeOH (9/1, v/v)[47] for 120 min at 20 °C, followed by *N*-acetylation with acetic anhydride in alkaline medium.[46,47] The *N*-acetylation degree was determined by integration of ^{13}C NMR signals at 60 and 55 ppm corresponding to the C-2 of $GlcNSO_3$ and GlcNAc, respectively. The glycol-split derivative of ^{50}NA-H (^{50}NA-H-^{25}-gs, **20**) was obtained from **19** (1 g) dissolved in 50 mL of 0.1 M $NaIO_4$. The solution was stirred at 4 °C for 16 h in the dark. The reaction was stopped by adding 5 mL of ethylene glycol, and the solution was dialyzed. Solid sodium borohydride (500 mg) was added to the retentate solution under stirring in several portions. After 2−3 h the pH was adjusted to 3 with 0.1 M HCl, and the solution was neutralized with 0.1 M NaOH. After dialysis, **20** was recovered in a 46% yield by freeze-drying.

Computer Modeling of FGF2/Hexasaccharide Complexes. Mixed-mode Monte Carlo/stochastic dynamics (MC/SD) calculations[30] were performed on models of a heparin hexasaccharide (H-Hexa) and its glycol-split analogue (sU-Hexa) complexed with FGF2 (see the text). All calculations were carried out on hexasaccharide−FGF2 substructures including the saccharide and all the protein atoms within 15 Å of the ligand. In this way the saccharide atoms were considered as freely moving atoms, whereas protein atoms were anchored by a harmonic restraining force constant of 418 kJ/mol Å^2 at the perifery of the freely moving substructure. To lock the ligand at binding site distance, constraints were imposed between the binding disaccharide moiety and the amino acid residues interacting with it.[29] All calculations were carried out using the MACROMODEL 7.1 version of BATCHMIN on a SGO2 workstation. The force field used for energy minimization was AMBER*, which includes Homan's parameters for pyranose.[48] The GB/SA (generalized born/surface area) continuum water solvation model was used.[28] For both complexes 2 ns of MC/SD simulations were run using a constant temperature of 300 K with a bath thermal constant (τ) of 0.2 ps and a dynamic time step of 1.0 fs.

Cell Cultures. Fetal bovine aortic endothelial GM 7373 cells were grown in Eagle's minimal essential medium containing 10% fetal calf serum (FCS), vitamins, and essential and nonessential amino acids. CHO-K1 cells and A745 CHO cell mutants (kindly provided by J. D. Esko, University of Birmingham, AL) were grown in Ham's F 12 medium supplemented with 10% FCS. A745 CHO cells harbor a mutation that inactivates the xylosyltransferase that catalyzes the first sugar transfer step in GAG biosynthesis.[49] The A745 CHO *flg*-1A clone, bearing about 30 000 FGFR1 molecules per cell, was generated by transfection with the IIIc variant of murine FGFR1 cDNA. [49]

FGF2-Mediated Cell−Cell Adhesion Assay. This assay allows an indirect evaluation of the formation of the FGFR/FGF2/HSPG ternary complex and was performed as described.[25] Briefly, CHO-K1 cell monolayers were incubated with 3% glutaraldehyde in PBS for 2 h at 4 °C. Fixation was stopped with 0.1 M glycine, and cells were washed extensively with PBS. Then, A745 CHO *flg*-1A cells (52 000 cells/cm^2) were added to CHO-K1 monolayers in serum-free medium *plus* 10

mM EDTA with no addition of or with 30 ng/mL FGF2 in the absence or in the presence of increasing concentrations of the compound under test. After 2 h of incubation at 37 °C, unattached cells were removed by washing twice with PBS, and A745 CHO *flg*-1A cells bound to the cell monolayer were counted under an inverted microscope at 125× magnification. Data, in duplicates, represent the mean of the cell counts of three microscopic fields per sample chosen at random. Then, the dose causing 50% inhibition (ID_{50}) of the FGF2-mediated cell−cell adhesion measured in cell cultures incubated with FGF2 alone was calculated for each compound. Experiments were repeated twice with similar results. For each compound, ID_{50} values are the mean of at least two experiments and the variability never exceeded 50% of the mean value.

Endothelial Cell Proliferation Assay. Proliferation assay on GM 7373 cells was performed as described.[25] Briefly, cells were seeded at 70 000 cells/cm^2 in 24-well dishes. Plating efficency was higher than 90%. After overnight incubation, cells were incubated in fresh medium containing 0.4% FCS and 10 ng/mL FGF2. After 8 h, increasing concentrations of the compound under test were added to cell cultures without changing the medium. After 16 h, cells were trypsinized and counted in a Burker chamber. Data were expressed as percent of cell proliferation measured in cells treated with FGF2 alone, and ID_{50} values were calculated for each compound. Experiments were repeated three times with similar results. For each compound, ID_{50} values are the mean of three experiments and the variability never exceeded 30% of the mean value.

Chick Embryo Chorioallantoic Membrane (CAM) Assay. Fertilized White Leghorn chick eggs were incubated under conditions of constant humidity at 37 °C. On the third day of incubation, a square window was opened in the egg shell after removal of 2−3 mL of albumen so as to detach the developing CAM from the shell. The window was sealed with a glass of the same size and the eggs were returned to the incubator. At day 8, 1 mm^3 sterilized gelatin sponges (Gelfoam, Upjohn Co., Kalamazoo, MI) adsorbed with the test compound (100 μg/embryo) dissolved in 5 μL of PBS were implanted on the top of growing CAMs (10 eggs/sample) under sterile conditions.[26] CAMs were examined daily under a stereomicroscope. On day 12, blood vessels entering the sponges within the focal plane of the CAM were recognized macroscopically at 50× magnification and counted by two observers in a double-blind fashion.[25] Data were expressed as percent of inhibition of vascularization in treated CAMs compared to control CAMs implanted with sponges containing vehicle alone. For each compound, data are the mean of at least two experiments (up to five experiments for the most active compounds), and variability never exceeded 20% of the mean value.

Appendix

Abbreviations: FGF2, fibroblast growth factor-2; GAG, glycosaminoglycan; VEGF, vascular endothelial growth factor; FGFR, tyrosine kinase FGF receptor; HS, heparan sulfate; HSPG, heparan sulfate proteoglycan; GlcA, β-D-glucuronic acid; IdoA, α-L-iduronic acid; GlcN, α-D-glucosamine; GlcNAc, *N*-acetyl-α-D-glucosamine; NS, *N*-sulfated regions; NA, *N*-acetylated regions; NA/NS, mixed regions; $GlcNSO_36SO_3$, α-D-glucosamine *N*,6-*O*-sulfate; $IdoA2SO_3$, α-L-iduronic acid 2-*O*-sulfate; $GlcN,3,6SO_3$, α-D-glucosamine *N*,3,6-*O*-sulfate; CAM, chick embryo chorioallantoic membrane; MW, weight average molecular weight; Pd, polydispersion; DS, sulfation degree; GPC−HPLC, gel-permeation chromatography−high-performance liquid chromatography; RI, refractive index; NMR, nuclear magnetic resonance spectroscopy; 1D, one-dimensional; 2D, two-dimensional; COSY, correlation spectroscopy; TOCSY, total correlation spectroscopy; MALDI-MS, matrix-assisted laser desorption ionization−time-of-flight−mass spectrometry; FCS, fetal calf serum; GalA, α-L-galacturonic acid; sU, glycol-split uronic acid; PST, pentasulfated trisaccharide; R, remnant of a hydrolyzed glycol-split residue; LMWH, low-molecular weight heparin; vLMWH, very low molecular weight heparin; MC/SD, Monte Carlo/stochastic dynamics; de, degree of epoxidation; gs, glycol splitting; H-Hexa, heparin hexasaccharide; sU-Hexa, heparin hexasaccharide with a glycol-split uronic acid unit.

Acknowledgment. This work was supported in part by grants from Associazione Italiana per la Ricerca sul Cancro, Ministero dell'Università e dalla Ricerca Scientifica e Tecnologica (Cofin 2002 and Centro di Eccellenza "IDET") to M.P.

References

(1) Kerbel, R.; Folkman, J. Clinical translation of angiogenesis inhibitors. *Nature Rev./Cancer* **2002**, *2*, 727−739.
(2) Bernfield, M.; Gotte, M.; Park, P. W. Function of cell surface heparan sulfate proteoglycans. *Annu. Rev. Biochem.* **1999**, *68*, 729−777.
(3) Iozzo, R. V.; San Antonio, J. D. Heparan sulfate proteoglycans: Heavy hitters in the angiogenesis arena. *J. Clin. Inv.* **2001**, *108*, 349−355.
(4) Sasisekharan, R., Shriver, Z.; Venkataraman, G.; Narayanasami, U. Roles of heparan sulfate glycosaminoglycans in cancer. *Nature Rev./Cancer* **2002**, *2*, 521−528.
(5) Fareed, J.; Hoppensteadt, D. A.; Bick, R. L. An update on heparins at the beginning of the new millennium. *Seminars Thromb. Hemost.* **2000**, *26* (1), 5−21.
(6) Smolenburg, S.; Van Noorden, C. J. The complex effects of heparins in cancer progression and metastasis in experimental studies. *Pharmacol. Rev.* **2001**, *53*, 93−105.
(7) Vlodavsky, I.; Friedman, Y.; Elkin, M.; Aingorn, H.; Atzmon, R.; Ishai-Michaeli, R.; Bitan, M.; Pappo, O.; Petretz, T.; Michal, I.; Spector, L.; Pecker, I. *Nature Med.* **1999**, *5*, 793−802.
(8) Borsig, L.; Wong, R.; Feramisco, J.; Nadeau, D. R.; Varki, N. M.; Varki, A. Heparin and cancer revisited: Mechanistic connections involving platelets, carcinoma mucins, and tumor metastasis. *Proc. Natl. Acad. Sci. U.S.A.*, **2001**, *98*, 3352−3357.
(9) Lapierre, F.; Holme, K.; Lam, L.; Tressler, L. J.; Storm, N.; Wee, J.; Stack, R. J.; Castellot, J.; Tyrrell, D. J. Chemical modifications of heparin that diminish its anticoagulant but preserve its heparanase-inhibitory, angiostatic, antitumor and anti- metastatic properties. *Glycobiology* **1996**, *6*, 355−366.
(10) Casu, B.; Lindahl, U. Structure and biological interactions of heparin and heparan sulfate. *Adv. Carbohydr. Chem. Biochem.* **2001**, *57*, 159−206.
(11) Capila, I.; Linhardt, R. J. Heparin-protein interactions. *Angew. Chem.(Int. Ed.)* **2002**, *41*, 390−412.
(12) Cross, M. J.; Claesson-Welsh, L. FGF and VEGF function in angiogenesis: Signaling pathways, biological responses and therapeutic inhibition. *Trends Pharmacol. Sci.* **2001**, *22*, 201−207.
(13) Coltrini, D.; Rusnati, M.; Zoppetti, G.; Oreste, P.; Isacchi, A.; Caccia, P.; Bergonzoni, L.; Presta, M. Biochemical bases of the interaction of human fibroblast growth factor with glycosaminoglycans. *Eur. J. Biochem.* **1993**, *214*, 51−58.
(14) Pellegrini, L. Role of heparan sulfate in fibroblast growth factor signaling: A structural view. *Curr. Opin. Struct. Biol.* **2001**, *11*, 629−634.
(15) Guimond, S.; Maccarana, M.; Olvin, B. B.; Lindahl, U.; Rapraeger, A. C. Activating and inhibitory heparin sequences for FGF-2 (basic FGF). *J. Biol. Chem.* **1993**, *268*, 23906−23914.
(16) Ornitz D. M.; Herr A. B.; Nilsson, M.; Westman, J.; Svahn, C.-M.; Waksman, G. FGF binding and FGF receptor activation by synthetic heparan-derived di- and trisaccharides. *Science* **1995**, *268*, 432−436.
(17) Lundin, L.; Larsson, H.; Krueger, J.; Kanda, S.; Lindahl, U.; Salvimirta, M.; Claesson-Welsh, L. Selectively desulfated heparin inhibits fibroblast growth factor- induced mitogeneity and angiogenesis. *J. Biol. Chem.* **2000**, *275*, 24653−24660.
(18) Jaseja, M.; Rej, R. N.; Sauriol, F.; Perlin, A. S. Novel regio- and stereoselective modifications of heparin in alkaline solution. Nuclear magnetic resonance spectroscopic evidence. *Can. J. Chem.* **1989**, *67*, 1449−1456.
(19) Rej, R. N.; Perlin, A. S. Base-catalyzed conversion of the α-L-iduronic acid 2-sulfate unit into a unit of α-L-galacturonic acid, and related reactions. *Carbohydr. Res.* **1990**, *200*, 427−447.

(20) Piani, S.; Casu, B.; Marchi, E. G.; Torri, G.; Ungarelli, F. Alkali-induced optical rotation changes in heparins and heparan sulfates, and their relation to iduronic acid-containing sequences. *J. Carbohydr. Chem.* **1993**, *12*, 507−521.
(21) Casu, B.; Diamantini, G.; Fedeli, G.; Mantovani, M.; Oreste, P.; Pescador, R.; Porta, R.; Torri, G.; Zoppetti, G. Retention of antilipemic activity by nonanticoagulant periodate-oxidized heparins. *Arzneim-Forsch. (Drug Res.)* **1986**, *36*, 637−642.
(22) Casu, B.; Guerrini, M.; Naggi, A.; Perez, M.; Torri, G.; Ribatti, D.; Carminati, P.; Giannini, G.; Penco, S.; Pisano, C.; Belleri, M.; Rusnati, M.; Presta, M. Short heparin sequences spaced by glycol-split uronate residues are antagonists of fibroblast growth factor-2 and angiogenesis inhibitors. *Biochemistry* **2002**, *41*, 10519−10528.
(23) Guerrini, M.; Bisio, A.; Torri, G. Combined quantitative ^{1}H and ^{13}C nuclear magnetic resonance spectroscopy for characterization of heparins. *Seminars Thromb. Hemost.* **2001**, *27*, 473−482.
(24) Linker, A.; Hovingh, P. Degradation of heparin as a tool for structural analysis. In *Heparin: Structure, cellular functions, and clinical applications;* McDuffie, N. M., Ed.; Academic Press: New York, 1979, pp 3−24.
(25) Leali, D.; Belleri, M.; Urbinati, C.; Coltrini, D.; Oreste, P.; Zoppetti, G.; Ribatti, D.; Rusnati, M.; Presta, M. Fibroblast growth factor-2 antagonist activity and angiostatic capacity of sulfated *Escherichia coli* K5 polysaccharide derivatives. *J. Biol. Chem.* **2001**, *276*, 37900−37908.
(26) Ribatti, D.; Goulandris, A., Bastaki, M., Vacca, A., Iurlaro, M.; Roncali, L.; Presta, M. New model of angiogenesis and antiangiogenesis in the chick embryo chorioallantoic membrane: The gelatin sponge/chorioallantoic membrane assay. *J. Vasc. Res.* **1997**, *34*, 455−463.
(27) Ribatti, D.; Urbinati, C.; Nico, B.; Rusnati, M.; Roncali, L.; Presta, M. Endogeneous basic fibroblast growth factor is implicated in the vascularization of the chick embryo chorioallantoic membrane. *Dev. Biol.* **1995**, *170*, 39−49.
(28) Still, W. C.; Tempczyk, A.; Hawlely, R.; Hendrickson, T. A general treatment of solvation for molecular mechanics. *J. Am. Chem. Soc.* **1990**, *112*, 6127−6129.
(29) Faham, S.; Hileman, R. E.; Fromm, J. R.; Linhardt, R. J.; Rees, D. C. Heparin structure and interactions with basic fibroblast growth factor. *Science* **1996**, *271*, 1116−112.
(30) Guarnieri, F.; Still, W. C. A rapidly convergent simulation method: Mixed Mo Carlo/Stochastic Dynamics. *J. Comput. Chem.* **1994**, *15*, 1302−1310.
(31) Plotnikov, A. N.; Schlessinger; J., Hubbard; S. H., Mohammadi, M. Structural basi for FGF receptor dimerization and activation. *Cell* **2000**, *9*, 413−424.
(32) Stauber, D. J.; Di Gabriele; A. D., Hendrikson, W. A. Structural interactions of fibroblast growth factor receptor with its ligands. *Proc. Natl. Acad. Sci. U.S.A.* **2000**, *97*, 49−54.
(33) Casu, B. Structure, shape and functions of glycosaminoglycans. In *New Trends in Hemostasis;* Harenberg, J., Heene, D. L., Stehle, G., Schettler, G., Eds.; Springer Verlag: Heidelberg, 1990; pp 2−11.
(34) Naggi, A.; Perez, M.; Torri, G.; Penco; S., Pisano; C., Giannini, G.; Vlodavsky, I.; Casu, B. *Commun. XXI Intern. Carbohydr. Symposium*, Cairns, 2002.
(35) Holme, K. R.; Liang, W.; Yang, Z.; Lapierre, F.; Shaklee, P. N.; Lam, L. A detailed evaluation of the structural and biological effects of alkaline 2-O-desulfation reactions of heparin. In *Nonanticoagulant action of glycosaminoglycans*; Harenberg, J.; Casu, B., Eds; Plenum Press: New York, 1996; pp 139−162.
(36) Conrad, H. E.; Guo, Y. Structural analysis of periodate oxidized heparin. In *Heparin and related polysaccharides;* Lane, D. A., Björk, I., Lindahl, U., Eds.; Plenum Press: New York, 1992; pp 31−36.
(37) Pisano, C.; Foderà R.; Marcellini M.; Giordano V.; Cervoni M. L.; Chiarucci, I.; Penco, S.; Riccioni, T.; Vesci, L.; Carminati, P. Antiangiogenic and antitumoral activity of novel heparin derivatives devoid of anticoagulant effects. *14th EORTC NCI-AACR Symposium* 2002, A 229.
(38) Isacchi, A.; Statuto, M.; Chiesa, L.; Bergonzoni, L.; Rusnati, M.; Sarmietos, P.; Ragnotti, G.; Presta, M. A six-amino acid deletion in basic fibroblast growth factor dissociates its mitogenic activity from its plasminogen activator-inducing capacity. *Proc. Natl. Acad. Sci. U.S.A.* **1991**, *88*, 2628−2632.
(39) Harenberg, J.; De Vries, J. X. Characterization of heparins by high-pressure size- exclusion liquid chromatography. *J. Chromatogr.* **1983**, *261*, 287−292.
(40) Wessler, E. Electrophoresis of acidic glycosaminoglycans in hydrochloric acid: A micro method for sulfate determination. *Anal. Biochem.* **1971**, *41*, 67−69.
(41) Keary, C. M. Charaterization of Methocel cellulose ethers by aqueous SEC with multiple detectors. *Carbohydr. Polym.* **2001**, *45*, 293−303.
(42) Casu, B.; Gennaro, U. A simple conductometric method for determining the sulfate and carboxylate groups in heparins and chondroitin sulfates. *Carbohydr. Res.* **1975**, *39*, 168−176.
(43) G. Venkataraman; Z. Shriver; Davis, J. C.; Sasisekharan, R. Fibroblast growth factors 1 and 2 are distinct in oligomerization in the presence of heparin-like glycosaminoglycans. *Proc. Natl. Acad. Sci. U.S.A.* **1999**, *96*, 1892−1897.
(44) Cifonelli, J. C. Reaction of heparitin sulfate with nitrous acid. *Carbohydr. Res.* **1968**, *8*, 233−242.
(45) Hoffman, J.; Larm, O.; Scholander, E. A new method for covalent coupling of heparin and other glycosaminoglycans to substances containing primary amino groups. *Carbohydr. Res.* **1983**, *117*, 328−331.
(46) Inohue, Y., Nagasawa, K. Selective N-desulfation of heparin with dimethylsulphoxide containing water or methanol. *Carbohydr. Res.* **1976**, *46*, 87−95.
(47) Nagasawa, K.; Inoue, Y.; Kamata, T. Solvolytic desulfation of glycosaminoglycuronan sulfates with dimethyl sulphoxide containing water or methanol. *Carbohydr. Res.* **1977**, *58*, 47−55.
(48) Homans, S. W. A molecular mechanical force field for the conformational analysis of oligosaccharides: Comparison of theoretical and crystal structures of Man-α1,3-Man-β1,4-GlcNAc. *Biochemistry* **1990**, *29*, 9110−9118.
(49) Esko, J. D. Genetic analysis of proteoglycan structure, function and metabolism. *Curr. Opin. Cell. Biol.* **1991**, *3*, 805−816.

JM030893G